



## A novel adjustable aperture for beam current controlling at China-ADS low energy beam transport line

Niu Haihua<sup>1,2</sup>, Li Youtang<sup>1</sup>, He Yuan<sup>2</sup>, Zhang Bin<sup>2</sup>, Wang Zhijun<sup>2</sup>, Chen Weilong<sup>2</sup>, Yuan Chenzhang<sup>2</sup>, Jia Huan<sup>2</sup>

(1. Lanzhou University of Technology, Lanzhou 730050, China;

2. Institute of Modern Physics, Chinese Academy of Sciences, Lanzhou 730000, China)

**Abstract:** A novel adjustable aperture is developed for the low energy beam transport line (LEBT) of the China Accelerator Driven Subcritical System (C-ADS). Two relatively rotating mirror-symmetry cores are adopted for the adjustable aperture to scrape unwanted outer particles, improve the beam quality and reduce the beam losses, and most of all, realize continuously tunable beam current and meet the requirement of round beam. The results of simulation and test show that the unwanted outer particles can be cut away and the beam current can be adjusted continuously online within the range of 0 to 10 mA. This device provides a convenient beam tuning method for the proton linear accelerator, which can satisfy the stable and reliable online operation of C-ADS linear accelerator.

**Key words:** adjustable aperture; beam commissioning; LEBT; C-ADS

**CLC number:** TL5 **Document code:** A **doi:** 10.11884/HPLPB202032.190393

At 2011, Chinese Academy of Sciences (CAS) started the “Strategic Priority Research Program (Category A)” project named “Future Advanced Nuclear Fission Energy”<sup>[1]</sup>. After six years of unremitting efforts, the China Accelerator Driven Subcritical System (C-ADS) team has made several significant breakthroughs of key technologies in the three major systems: the high current superconducting proton linear accelerator, the heavy metal spallation target and the subcritical reactor. The high-current superconducting proton linear accelerator is mainly composed of an electron cyclotron resonance ion source (ECR), a low energy beam transport line (LEBT), a radio frequency quadrupole (RFQ), a medium energy beam transport line (MEBT), a superconducting RF cavity accelerating section (SC section) and a high energy beam transport line (HEBT)<sup>[2-3]</sup>.

LEBT is one of the key components of C-ADS proton linac. It starts from the exit of the ECR and ends with the RFQ entrance. LEBT mainly consists of two groups of solenoid with two steering magnets, two diagnostic chambers, a limited cone, an electron trap, and a beam chopper<sup>[4]</sup>, it can effectively transmit the 35 keV and 10 mA proton beam from the ECR to the entrance of the RFQ and achieve the optical matching to the RFQ.

During the online beam commissioning of the superconducting cavity from low power to high power in the continuous-wave (CW) mode, the beam from the ECR is required to be continuously adjustable. In addition, the focusing of solenoid at the LEBT requires a round beam and the aberrations of the solenoid to the beam should be eliminated<sup>[5-6]</sup>. In order to satisfy these requirements, a novel adjustable aperture for C-ADS LEBT was developed. There are several similar devices with different structure used at European Spallation Source (ESS) and the Soreq Applied Research Accelerator Facility (SARAF). A six movable blades iris with an adjustable aperture was adopted to control beam current in the LEBT at ESS. Its beam aperture is from 1 mm to 80 mm with hexagonal shape<sup>[7-8]</sup>. A variable diameter aperture is used during beam operation to cut away unwanted outer particles and decrease the beam current continuously at SARAF LEBT<sup>[9-11]</sup>. Compared to these devices, the most significant improvements of our adjustable aperture for C-ADS LEBT are that it is compact in structure and it can change the beam current continuously in the whole range down to zero, and satisfy the round beam requirement at the same time.

\* Received date: 2019-09-30; Revised date: 2020-02-15

**Foundation item:** Strategic Priority Research Program of Chinese Academy of Sciences (XDA21010202)

**Biography:** Niu Haihua (1987 —), female, PhD candidate, engaged in the research on mechanical equipment of linear accelerator; niuhh@impcas.ac.cn.

**Corresponding author:** He Yuan (1973—), male, PhD, engaged in the research on physics and technology of high power superconducting linear accelerator; hey@impcas.ac.cn

## 1 The principle and structure design of the adjustable aperture

Beam matching between different acceleration segments is important to reduce beam losses and emittance growth. The mismatch from the LEBT is one of the main sources of beam losses in the RFQ. The beam losses lead to the thermal deformation of the RFQ electrode surface and then causes radio frequency arcing, which reduces the stability of the long-term operation of the RFQ<sup>[12]</sup>. Since the confining magnetic field of the ECR is axisymmetric, the beam from ECR is also considered an axisymmetric round beam. The diameter of beam spot is less than 40 mm. To better meet the requirements of physical and optical matching for the RFQ, an adjustable aperture should be designed at the LEBT to achieve continuous tuning of beam current in the entrance of the RFQ, and satisfy the stable and reliable online operation of the C-ADS linear accelerator. The following are the key points:

- 1) The adjustable aperture needs to satisfy the round beam.
- 2) The beam current can be adjusted continuously on line.
- 3) Although for the beam commissioning, the beam power at the LEBT was determined to be 350 W (35 keV, 10 mA), the adjustable aperture should be able to withstand a heat load of 1 kW to allow for equipment upgrades in future.

Based on the above requirements, a novel core component of the adjustable aperture with cooling water made of 304 stainless steel was designed, the schematic diagram of the core component is shown in Fig. 1. It contains two cylindrical rotating cores which are mirror symmetric to each other. Each core has a water-cooled tubing in the center and a cylinder with a series of half-moon shaped grooves, as shown in Fig.1(a). With the half-moon shape grooves opening perfectly matched, the two pillars sitting together are able to produce a circular aperture in between. As shown in Fig.1(b), on the pillar from the azimuth angle  $0^\circ$  to  $190^\circ$ , the diameter of the half moon shape groove increases from 2 mm to 40 mm continuously. Therefore the aperture's diameter is continuously tunable to meet the needs of beam tuning. While from the azimuth angle  $190^\circ$  to  $270^\circ$ , the diameter of the half moon shape groove remains at 40 mm. The aperture will be completely closed when the azimuth angle is between  $270^\circ$  and  $360^\circ$ , and then the continuous adjustment of the beam current from 10 mA down to 0 mA is achieved.

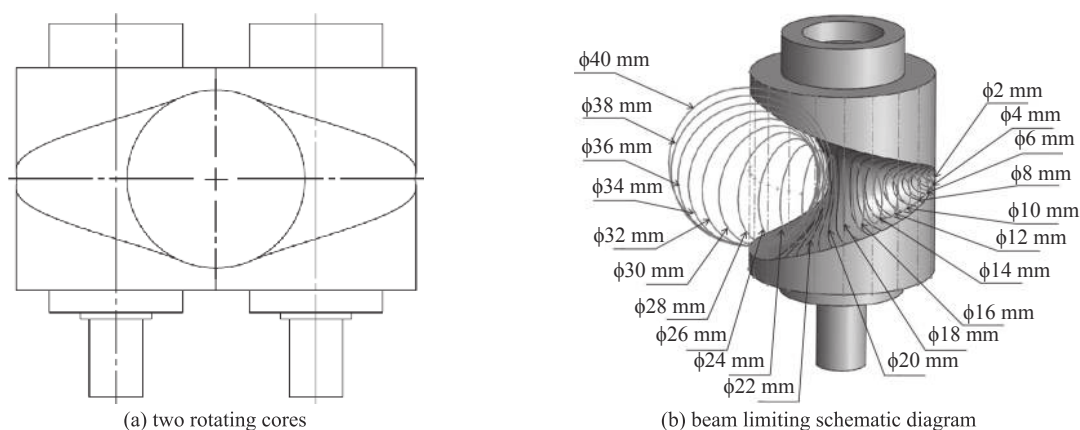


Fig. 1 The schematic diagram of the core component for adjustable aperture

The adjustable aperture is scheduled to install on the CF100 flange of C-ADS LEBT test chamber. The whole aperture structure is very compact and includes a CF100 flange, a bearing seat, a support frame, two rotating cores, water-cooling stepped shaft components and driving parts. The detailed structure is shown in Fig. 2(a), the adjustable aperture is characterized by compact structure, high adjustment accuracy, stability and reliability, easy installation, and the high power beam current effectively controlled with high precision.

### 1.1 Vacuum seal

The operation of the accelerator is inseparable from the vacuum environment. Thus, the assembly of adjustable aperture to vacuum chamber must meet the high vacuum requirement for accelerator, and the vacuum inside the LEBT should be  $10^{-4} \sim 10^{-5}$  Pa. Since the two stepped shafts of the aperture transfer relative rotation from the atmosphere to the vacuum

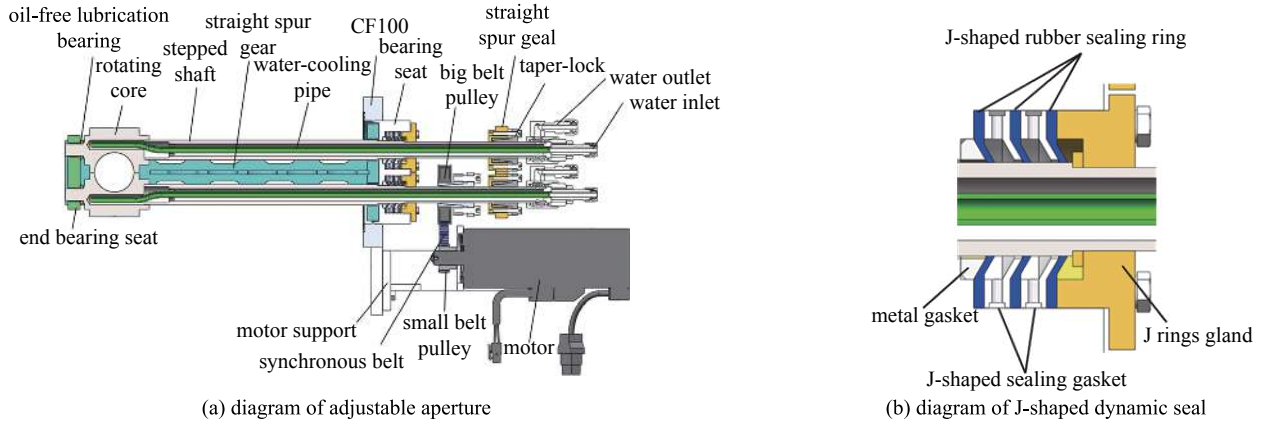


Fig. 2 The structure diagram of the adjustable aperture

chamber, the design for a dynamic seal for such high vacuum is always challenging. As a solution, a J-shaped dynamic seal structure was adopted, as shown in Fig. 2(b), and it is composed of a metal gasket, three J-shaped rubber sealing rings, two J-shaped sealing gaskets and a J rings gland.

### 1.2 Actuating device

The actuating device consists of a servo motor, an absolute rotary encoder, a synchronous pulley, a synchronous belt, a taper-lock, a straight spur gear and a transmission shaft. The servo motor transmits the power to the transmission shaft through synchronous belt, the taper-locks are installed on the transmission shafts, and the taper-locks are equipped with gears, which drive the mirror rotation of the transmission shafts through gear engagement. The rotation of the rotating cores is under control of servo motor, the system adopts closed-loop control, the positioning accuracy of rotation can be 0.5° without repeating location accumulation error.

### 1.3 Design and strength analysis of support

The support is bolted onto the CF100 flange for supporting and fastening the adjustable aperture components. Its material is 304 stainless steel, the thickness of the round plate on the mounting surface, the side plates, the middle rib plate and the end bearing seat are 12 mm, 6 mm, 4 mm and 12 mm, respectively. The load of the support mainly comes from its own weight, the weight of two rotating cores, and the weight of the water-cooling shaft components. According to the statics analysis and calculation, the equivalent weight on the support is about 6 kg, and the static load is about 60 N. The end bearing seat is connected to the ends of two side plates by screws. Its loads consist of radial pressure  $p_1$  and uniform axial pressure  $p_2$  and concentrate on the two bearing bores.  $p_0$  is the uniform radial load of two bearing bores. The specific calculation is shown in the following three equations.

$$p_0 = 2F_r / (\pi r b) \tag{1}$$

$$p_1 = 0.75 p_0 \tag{2}$$

$$p_2 = 0.2 p_0 \tag{3}$$

Where  $F_r$  is the radial resultant force on the bearing bore,  $r$  is the radius of the bearing bore,  $b$  is the thickness of the bearing bore. Calculated results show that  $p_0$  is 0.45 MPa,  $p_1$  is 0.34 MPa and  $p_2$  is 0.09 MPa. The support structure was analyzed using ANSYS Workbench software. Fig. 3 shows the maximum deformation is about 0.08 μm. The results indicate that such a support made of 304 stainless steel is strong enough to hold the entire structure.

### 1.4 Thermo-mechanical analysis and manufacturing

The proton beam bombards the rotating cores and the beam

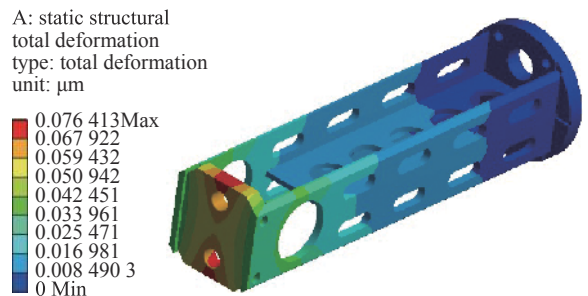


Fig. 3 ANSYS simulation result of support

power is dissipated on them as heat. Without proper cooling, the temperature of the rotating cores would rise continuously and eventually cause the deformation of the rotating cores. Due to the tight fitting between the two cores, thermal deformation will cause the two cores to be stuck and unable to rotate. Thus, it is important to analyze the heat flow on the cores with the beam power and water cooling taken into consideration.

On the transverse directions, the proton beam from ECR of C-ADS proton linac follows the Gaussian distribution. Calculated by the software SRIM, it was found that the penetration depth of 35 keV proton beam in 304 stainless steel is about 0.2 μm. Therefore it can be assumed that the beam power would be completely deposited on the surface of the rotating cores. The Gaussian surface heat source model is used as the heat source model of the proton beam bombarding the cores, the expression is

$$q(r) = \left[ 3P / (\pi R^2) \right] \exp(-3r^2/R^2) \quad (4)$$

where  $q(r)$  is the heat flow of formation at radius  $r$ ,  $P$  is beam power,  $R$  is beam spot radius.

Reynolds number is the characterization for the dimensionless number of fluid flow situation, used to determine laminar or turbulent, as

$$Re = \rho v d / \mu \quad (5)$$

where  $\rho$  is fluid density,  $v$  is fluid flow velocity,  $d$  is the channel diameter and  $\mu$  is viscosity coefficient.

The average speed of cooling water flow in the LEBT is 3 m/s, resulting in a turbulent flow in the water pipe. In this case, ANSYS Fluent was employed to calculate the cooling process, and the standard  $k-\epsilon$  model in the turbulence model analysis was used for simulation.

In the worst scenario, the boundary conditions for heat simulation go as follows: 1) The beam power is 1 kW (current value is 350 W, may upgrade to 1 kW in the near future); 2) The 3 times of RMS beam radius is 20 mm, the aperture is completely closed; 3) The water temperature at inlet is 20 °C; 4) The average velocity of cooling water is 3 m/s; 5) The Gaussian heat source distribution was added with user-defined program UDF.

As shown in Fig. 4(a), the maximum temperature on the core is 975.4 K and far below the melting point of 304 stainless steel. Based on the calculation result, the thermal deformation of the core was calculated by ANSYS fluid-solid coupling. As shown in Fig. 4(b), the maximum thermal deformation is 0.08 mm. The actual assembly clearance between the two cores is designed to be 0.2 mm, leaving space for the thermal deformation, and guaranteeing safe and stable operation of the rotating cores in the long run.

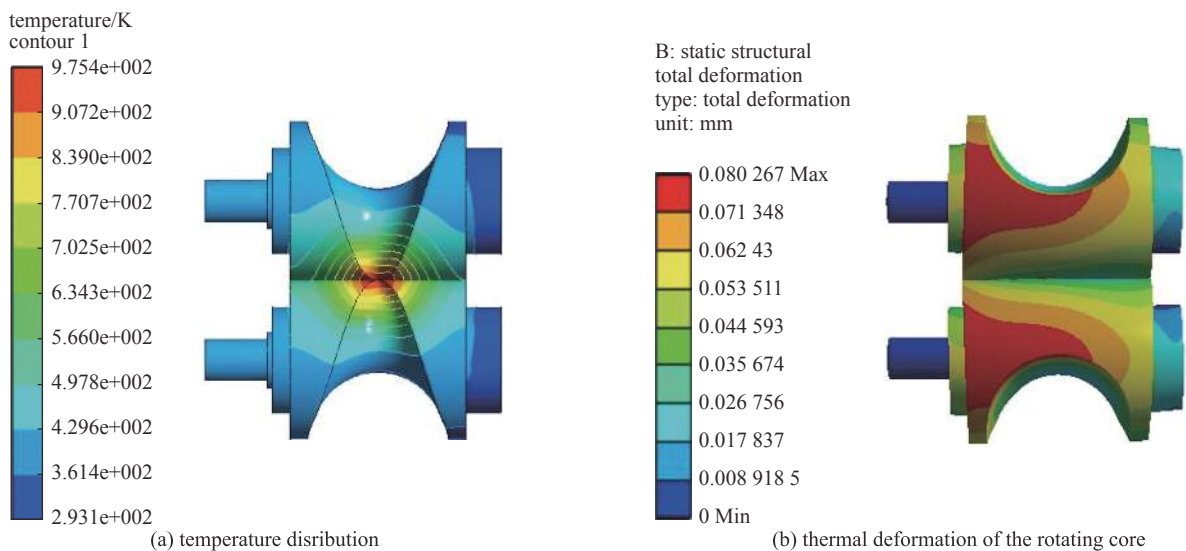


Fig. 4 Temperature distribution and thermal deformation of the rotating core

## 2 Simulation and test of the adjustable aperture

For the superconducting linear accelerator of C-ADS, it is necessary to realize beam commissioning from low power to high power in CW mode. In practice, increasing the beam loading from low beam current to high beam current is an effective

commissioning scheme. The LEBT is the main section for controlling the beam current and beam quality, the beam dynamics of the LEBT was studied in Ref.[13]. It appears obviously that there are beam tails in the phase space at the exit of the LEBT, and the analysis shows that the beam tails mainly come from aberration of solenoids. In the simulation, the aberration effect can be reduced if an adjustable aperture was placed in front of the solenoid to optimize the beam envelope, which can effectively improve the beam quality.

### 2.1 Simulation of the adjustable aperture

The beam dynamics simulation of the LEBT with aperture in the CW mode was carried out. The adjustable aperture was located at the 0.6 m of the LEBT from the ion source beam extraction aperture. The space charge compensation (SSC) was considered in beam dynamics simulation, and the SSC factor was 90%. In Fig. 5, the upper panel of Fig. 5(a) shows the 3RMS envelope in the  $X$  direction, the lower panel of Fig. 5(a) shows the 3RMS envelope in the  $Y$  direction. Since the LEBT uses two solenoids to focus the beam from ECR to RFQ, the beam envelopes in the  $X$  and  $Y$  directions are identical. Because of the space charge effect among the beam particles, which is stronger for low-energy particles due to the low transmission speed, the beam particles tend to diverge, and an external magnetic field is required to focus the beam. The beam reduction of LEBT with adjustable aperture is shown in Fig. 5 (b), nearly 24% of the beam is cut away by the aperture in this simulation, this illustrates the adjustable aperture can play a good role in scraping unwanted beam particles.

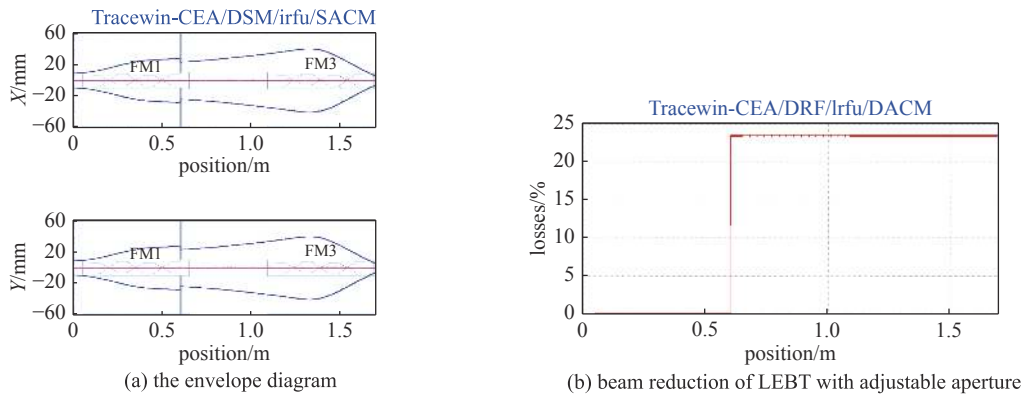


Fig. 5 The envelope diagram and beam reduction of LEBT with adjustable aperture

The beam phase space and real space plots at the adjustable aperture are shown in Fig. 6. Because the aperture is roughly circular, the phase space plots shows that it can scrap part of the outer particles of the  $X-X'$ ,  $Y-Y'$  in phase space, keeping the phase diagram basically unchanged and the beam parameters still match to the acceptance of RFQ. The red dots depict the scraped outer particles.

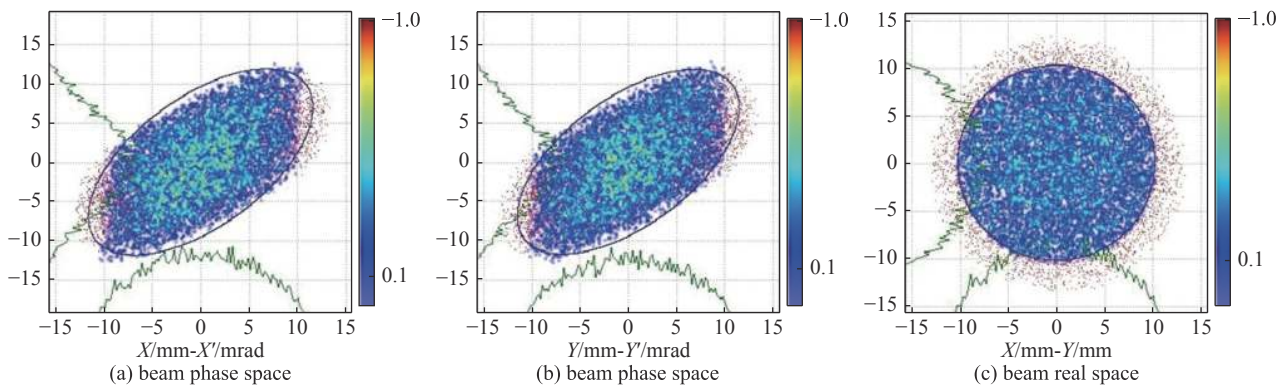


Fig. 6 Beam phase space and real space plots at the adjustable aperture

The beam parameters at the outlet of the LEBT are shown in Table 1, which shows that the beam parameters have changed slightly after the beam scraping, thus the beam can still be well matched to RFQ. At the same time, the normalized RMS emittance is significantly reduced. By effectively reducing the geometrical emittance of the beam at the outlet of the LEBT, the transmission matching between LEBT and RFQ is more favorable. It can be seen from the simulation that the LEBT with

**Table 1** The beam parameters at the outlet of the LEBT

	emittance $\varepsilon_x/(\pi\cdot\text{mm}\cdot\text{mrad})$	Twiss $\alpha_x$	Twiss $\beta_x/[\text{mm}/(\pi\cdot\text{mrad})]$	emittance $\varepsilon_y/(\pi\cdot\text{mm}\cdot\text{mrad})$	Twiss $\alpha_y$	Twiss $\beta_y/[\text{mm}/(\pi\cdot\text{mrad})]$
before scraping	0.207	0.908	0.047	0.207	0.910	0.047
after scraping	0.173	1.120	0.058	0.173	1.110	0.058

aperture works well.

## 2.2 Test of the adjustable aperture

Fig. 7 is a picture of the adjustable aperture. Before installing the adjustable aperture onto LEBT, off-line debugging was performed, a series of divisions were engraved on the J rings gland of the aperture as seen in Fig. 8. The aperture diameter was expected to be in consistent with the size indicated by the pointer through debugging. After installing the adjustable aperture on LEBT, it was collimated with the beam orbit as the reference line to ensure that the true aperture diameter matches the value indicated by the pointer.

The actual beam transmission through the adjustable aperture was tested at the LEBT of C-ADS with continuous beam of 35 keV and 10 mA. The test site is shown in Fig. 8, the pressure in the beam pipe during the test was  $1.3\times 10^{-4}$  Pa. In this test, we selected every  $5^\circ$  as the measuring points, the beam current was measured for every  $5^\circ$  of rotation. As can be seen from the test results in Fig. 9, when the rotation angle of two rotating cores is  $190^\circ$ , the diameter of the aperture reaches its maximum, 40 mm. At this position, the beam pass rate and the beam current are the highest. Reducing the rotation angle of the cores, the beam current decreased with the reduction of the aperture diameter. Because of the gas injection state of the ion source, the beam current cannot reach 10 mA in this test, but our ion source has the extraction condition of 10 mA, it is noteworthy for the relationship between the aperture and beam current in the process of adjusting apertures. Coupled with the Faraday cup and DCCT(Direct Current-Current Transformer), the beam current can vary continuously within the range of 0 to 10 mA from the rotation angle  $0^\circ$  to  $190^\circ$ .

## 3 Conclusion

The mechanical design, simulation and test of an adjustable aperture, which will be installed in the low energy beam transport line of C-ADS, were performed at Institute of Modern Physics (IMP). The aperture structure is able to realize continuous modulation of beam current during the online accelerator tuning and to satisfy the round beam shape. The mechanical and heat analyses show the aperture is capable of long time stable operation under 1 kW CW proton beam. In general, this adjustable aperture provides a convenient beam tuning method for the proton linear accelerator, which can satisfy the stable and reliable operation of C-ADS linear accelerator online.

**Acknowledgements:** One of the authors Niu Haihua would express her sincere acknowledgement to the colleagues in IMP (Wu Qi, Wang Jing, Zhang Lei) and the beam-commissioning group of China-ADS Injector-II for their help in the adjustable aperture testing and beam commissioning. Special thanks go to Tan Teng for his advice on the paper work.



Fig. 7 The adjustable aperture



Fig. 8 Test site of the aperture

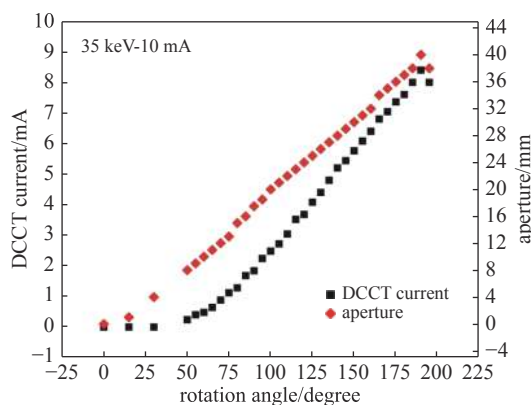


Fig. 9 Test results of the aperture

## 参考文献：

- [1] Zhan Wenlong, Xu Hushan. Advanced fission energy program-ADS transmutation system[J]. Bulletin of Chinese Academy of Sciences, 2012, 27: 375-381.
- [2] Wang Jing, Huang Jian-Long, He Yuan, et al. Multi-physics analysis of the RFQ for Injector Scheme II of C-ADS driver linac[J]. Chinese Physics C, 2014, 38(10): 107005.
- [3] Niu Haihua, Li Youtang, He Yuan, et al. The mechanical design and fabrication of 162.5 MHz buncher for China accelerator driven sub-critical system injector II[J]. Nuclear Engineering and Technology, 2017, 49: 1071-1078.
- [4] Wu Q, Zhang Z M, Sun L T, et al. A 2.45 GHz intense proton source and low energy beam transport system for China Initiative Accelerator Driven Sub-Critical reactor system[J]. Review of Scientific Instruments, 2014, 85: 02A703.
- [5] Yang Y, Zhang Z M, Wu Q, et al. A low energy beam transport system for proton beam[J]. Review of Scientific Instruments, 2013, 84: 033306.
- [6] Yang Yao, Zhang Zimin, Zhang Wenhui, et al. Study on beam emittance growth induced by spherical aberration of solenoid lens[J]. Atomic Energy Science and Technology, 2013, 47(12): 2336-2340.
- [7] Celona L, Allegra L, Amato A, et al. Preliminary commissioning results of the proton source for ESS at INFN-LNS[C]// Proc of IPAC. 2016: 2628-2631.
- [8] Eshraqi M, Danared H, Jansson A, et al. ESS linac beam physics design update[C]// Proc of IPAC. 2016: 947-950.
- [9] Weissman L, Berkovits D, Arenshtam A, et al. SARAF phase I linac in 2012[J]. Journal of Instrumentation, 2014, 9: T05004.
- [10] Kai D, Florian K, Christian P. Performance of the SARAF ion source[C]// Proc of PAC07, 2007, TUPAN009: 1407-1409.
- [11] Weissman L, Berkovits D, Eliyahu I, et al. The state of the SARAF LINAC Project[C]// Proc of LINAC. 2010: 679-683.
- [12] Wu Qi, Jia Huan, Ma Hongyi, et al. Research of emittance matching on the low energy beam transport line for ADS proton LINAC[J]. Nuclear Physics Review, 2015, 32: 5-9.
- [13] Chen Weilong. LEBT design based on beam loss control[D]. Beijing: University of Chinese Academy of Sciences, 2016.

# 一种用于 C-ADS 低能束流传输线束流强度控制的新型可调限束光阑

牛海华<sup>1,2</sup>, 李有堂<sup>1</sup>, 何源<sup>2</sup>, 张斌<sup>2</sup>, 王志军<sup>2</sup>, 陈伟龙<sup>2</sup>, 袁辰彰<sup>2</sup>, 贾欢<sup>2</sup>

(1. 兰州理工大学 机电工程学院, 兰州 730050; 2. 中国科学院 近代物理研究所, 兰州 730000)

**摘要：**为了实现超导直线加速器束流强度的连续可调，并满足加速器在线稳定可靠运行，针对我国加速器驱动次临界系统(C-ADS)低能束流传输线(LEBT)的束流强度调控，提出了一种新型的可调限束光阑。可调限束光阑采用两个相对旋转的镜像对称转芯，转芯的孔径在某一范围内可以实现连续变化，以刮除不必要的外部粒子，提高束流品质，降低束损，最重要的是可实现束流强度的在线连续可调，并满足圆形束的要求。仿真和试验结果表明，在0~10 mA范围内，可以有效地卡掉不必要的外部粒子束流，并实现束流强度的在线连续调节。该装置为质子直线加速器提供了一种方便的束流调试方法，能够满足ADS直线加速器稳定可靠的在线运行。

**关键词：**可调光阑；束流调试；低能束流传输线；中国加速器驱动次临界系统